

PROFESSOR YIPING CHEN (Orcid ID : 0000-0002-5198-3348)

DR XIANGDUAN TAN (Orcid ID : 0000-0001-8627-5483)

Article type : Research Article

Discovery of novel *N*-aryl pyrrothine derivatives as bacterial RNA polymerase inhibitors

Mo-Han Huang^{1,2}, Bo Kong³, Jie-Yun Meng¹, Yu-Bin Lv¹, Yan-Fen Peng¹, Yi-Ping Chen^{4,5,*}, Xiang-Duan Tan^{1,*}

¹ College of Pharmacy, Guilin Medical University, Guilin 541004, China

² Department of Pharmacy, Liuzhou People's Hospital, Liuzhou 545006, China

³ School of Life Sciences, Guangzhou University, Guangzhou, 510006, China

⁴ School of Pharmaceutical Sciences, Guangxi University of Chinese Medicine, Nanning 530200, China

⁵ Guangxi Key Laboratory of Translational Medicine for Treating High-Incidence Infectious Diseases with Integrative Medicine, Nanning 530200, China

□ Correspondence: E-mail: tandu@glmc.edu.cn (X.-D.T.); yipchen2009@foxmail.com (Y.-P.C).

Abstract:

This article has been accepted for publication and undergone full peer review but has not been through the copyediting, typesetting, pagination and proofreading process, which may lead to differences between this version and the [Version of Record](#). Please cite this article as [doi: 10.1111/CBDD.13736](#)

This article is protected by copyright. All rights reserved

Bacterial RNA polymerase (RNAP) is a validated drug target for broad-spectrum antibiotics, and its “switch region” is considered as the promising binding site for novel antibiotics. Based on the core scaffold of dithiolopyrrolone, a series of *N*-aryl pyrrothine derivatives was designed, synthesized and evaluated for their antibacterial activity. Compounds generally displayed more active against Gram-positive bacteria, but less against Gram-negative bacteria. Among them, compound **6e** exhibited moderate antibacterial activity against clinical isolates of rifampin-resistant *Staphylococcus aureus* with MIC value of 1-2 µg/mL, and inhibited *Escherichia coli* RNAP with IC₅₀ value of 12.0 ± 0.9 µM. In addition, compound **6e** showed certain degree of cytotoxicity against HepG2 and LO2 cells. Furthermore, molecular docking studies suggested that compound **6e** might interact with the switch region of bacterial RNAP in a similar conformation to myxopyronin A. Together, the *N*-aryl pyrrothine scaffold is a promising lead for discovery of antibacterial drugs acting against bacterial RNAP.

Keywords: dithiolopyrrolone, *N*-aryl pyrrothine, bacterial RNA polymerase, inhibitors, antibacterial activity

1 INTRODUCTION

Multiple drug resistant (MDR) bacteria are one of the most important threats to public health worldwide (Oliva et al., 2018), and lead to an increase in the number of infections and the costs associated with these infections (Pendleton et al., 2013; Rossolini et al., 2014). Bacterial RNA polymerase (RNAP) acts as a key enzyme in transcription regulation and gene expression (Mosaei & Harbottle, 2019), and is highly conserved among bacteria, but less highly conserved with eukaryotic RNAP sequences, which makes RNAP an excellent target for broad-spectrum antibacterial agent discovery (Ma, 2016). Rifampicin is the well-known clinical antibiotic targeting bacterial RNAP and has been the first line antibiotics used for tuberculosis treatment since 1970s (Chopra 2007; Villain et al., 2007). However, the emerging rifampin-resistant mycobacteria has threatened the usefulness of this drug in treating mycobacterial diseases (Campbell et al., 2001; Darst, 2004).

Dithiolopyrrolones are a class of antibiotics that possess the unique pyrrolinonodithiole (4*H*- [1,2] dithiolo [4,3-*b*] pyrrol-5-one) skeleton (Qin et al., 2013). Currently, there are approximately 30 naturally occurring dithiolopyrrolone derivatives identified, including thiolutin, holomycin, aureothricin, xenorhabdin I and thiomarinols (**Figure 1**) (Li et al., 2014; Gao et al., 2014; Maffioli et al., 2017). These derivatives belong to *N*-methyl, *N*-acyl pyrrothine (thiolutin type), *N*-acyl pyrrothine (holomycin type) and thiomarinols. Natural dithiolopyrrolones exhibit relatively broad-spectrum antibiotic activity against many Gram-positive and Gram-negative bacteria (Qin et al., 2013). In recent years, *N*-aryl pyrrothine derivatives have been reported to have anticancer (Li et al., 2007) and anti-leukopenia activity (Tan et al., 2013; Li et al., 2014).

Recently, the bacterial RNAP “switch region” was considered as a new binding site for drug discovery (Sahner et al., 2013). The “switch region” located at the base of the clamp serves as a hinge that facilitates the clamp swinging

between the open and closed state (Irschik et al., 1983). The switch region is distinct from the rifamycins binding site on RNAP and is highly conserved in Gram-positive and Gram-negative bacteria (Li et al., 2014). Myxopyronins, corallopyronins and ripostatins target the switch region of the bacterial RNAP and prevent extension of RNA during transcription initiation by restraining the entry of the promoter DNA, which interacts with RNAP (Figure 1) (Mukhopadhyay et al., 2008; Ho et al., 2009). Currently, natural dithiopyrrolone compounds, such as thiolutin and holomycin, show antibacterial activity that is attributed to the inhibition of RNA synthesis (Qin et al., 2013). The hybrid-type antimicrobial agent **29** also shows antibacterial activity, and might binds to be the switch region according to molecular docking studies (Yakushiji et al., 2013). Dithiopyrrolones derivatives are popular structures for developing the next generation of bacterial RNAP inhibitors (Qin et al., 2013).

Previous reports have not described the antibacterial activity of *N*-aryl pyrrothine derivatives. In this study, the core scaffold of natural pyrrothine was used as a template to do further structural optimization. A series of *N*-aryl pyrrothine derivatives was designed and synthesized (**Figure 2**), which bear the aryl group at the *N*-4 position, and a variety of alkyl or aromatic groups in the amino group at the *C*-6 position of the pyrrothine core scaffold, followed by structure-activity relationship study and biological evaluation.

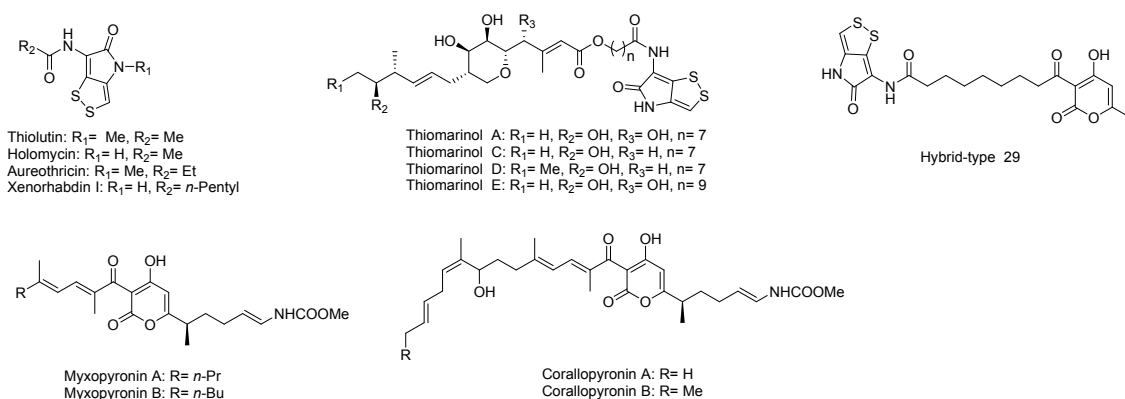


Figure 1. Chemical structures of dithiopyrrolones, myxopyronins and corallopyronins

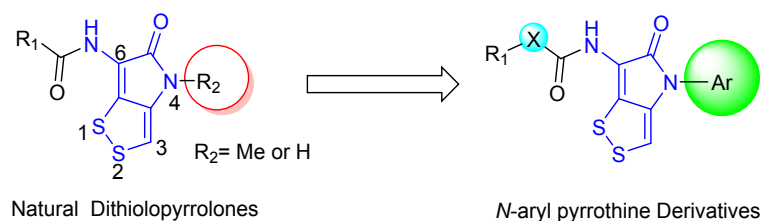


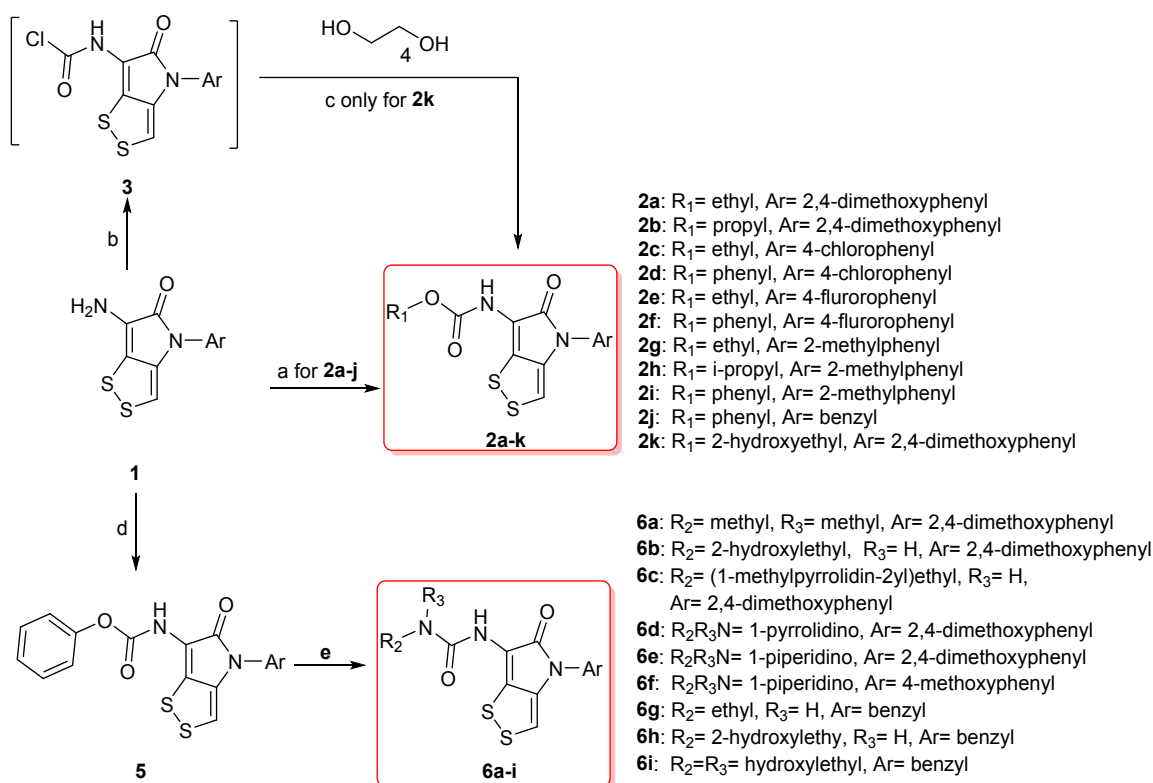
Figure 2. General design strategy for *N*-aryl pyrrothine derivatives.

2 RESULTS AND DISCUSSION

2.1 Chemistry Synthesis

The synthesis procedures for *N*-aryl pyrrothine derivatives is shown in **Scheme 1**, following the synthesis routes on previous reports with minor modifications (Tan et al., 2013; Li et al., 2014). The starting material of compound **1**

was obtained according to previous procedure (Tan et al., 2013). Compounds **2a–j** were synthesized from compound **1** and chlorocarbonate derivatives ($R_1\text{OCOCl}$) by amidation reaction at room temperature for 3–10 h. Treatment of compound **1** with triphosgene in the presence of THF afforded intermediate **3**, Glycol (**4**) was then reacted with intermediate **3** to obtain **2k**. Reaction of compound **1** with phenyl chloroformate at room temperature for 3–8 h afforded intermediate **5** (Thavonekham, 1997). Compounds **6a–i** were synthesized by nucleophilic substitution of compound **5** with the corresponding amines ($R_2R_3\text{NH}$) (Li et al., 2014). The synthesized compounds were confirmed by ^1H NMR, ^{13}C NMR and mass spectrometry (see Supporting information).



Scheme 1. Synthesis of *N*-aryl pyrrothine derivatives **2a–k** and **6a–i**. Reagents and conditions: (a) $R_1\text{OCOCl}$, Et_3N , THF, rt, 3–10 h, 45–63%; (b) triphosgene, THF, 0–5 °C, 1 h; (c) Et_3N , THF, 0 °C–rt, 2 h, 49% in two steps; (d) phenyl chloroformate, Et_3N , THF, rt, 3–8 h; (e) amines ($R_2R_3\text{NH}$), THF, rt, 8–12 h, 40–56% in two steps.

2.2 Biological Evaluation

2.2.1 Disk Diffusion Test

Disk diffusion test was used to assess antibacterial activity for all the synthesized compounds with rifampin and ciprofloxacin as positive controls. Paper wafer containing 30 μg of test compound was placed on Muller–Hinton agar plate where bacteria of *Staphylococcus aureus* (*S. aureus*) or *Escherichia coli* (*E. coli*) had been inoculated. The

diameter of the clear zones around the paper wafer was measured and shown in **Table 1**. Interestingly, all the compounds showed stronger inhibition against Gram-positive bacteria of *S. aureus* than the Gram-negative bacteria of *E. coli*. Among them, four compounds (**2k**, **6a**, **6e** and **6f**) exhibited strong activity against *S. aureus* (inhibition zone > 20 mm) than the other ten compounds (**2a**, **2b**, **2f**, **2g**, **2h**, **6b**, **6c**, **6d**, **6h** and **6i**) (16 mm < inhibition zone < 20 mm). All the synthesized compounds displayed weak activity against *E. coli* with an inhibition zone < 12 mm.

Table 1. Disk diffusion test using *S. aureus* and *E. coli*.

Compd.	Inhibition zone (mm) ^a		Compd.	Inhibition zone (mm) ^a	
	<i>S. aureus</i>	<i>E. coli</i>		<i>S. aureus</i>	<i>E. coli</i>
	ATCC 29213	ATCC 25922		ATCC 29213	ATCC 25922
2a	16.16	8.23	6a	20.23	9.34
2b	16.23	8.45	6b	19.62	9.02
2c	12.23	9.45	6c	18.23	9.14
2d	10.56	9.78	6d	18.46	8.70
2e	16.63	8.41	6e	23.34	8.39
2f	9.33	8.34	6f	20.83	8.51
2g	19.87	8.65	6g	11.82	8.54
2h	19.10	8.16	6h	19.16	8.25
2i	10.49	8.41	6i	18.84	8.36
2j	14.32	7.25	Rif ^b	36.16	17.20
2k	25.48	11.36	Cip ^b	33.42	38.84

^a The diameter of inhibition zones for compounds **2a–k** and **6a–i** in the disk diffusion test. All compounds were dissolved in MeOH and tested at a dose of 30 µg/wafer.

^b Used as a positive control. Rifampin (Rif), ciprofloxacin (Cip).

2.2.2 Determination of Minimum Inhibition Concentration (MIC)

An MIC assay against five bacteria was further performed for the compounds showing antibacterial activities in disk diffusion test (inhibition zone against *S. aureus* > 16 mm), and presented in Table 2. Compounds **2g**, **2k**, **6d**, **6e** and **6f** showed the lowest MIC value (1 µg/mL) against *S. aureus*, and four compounds (**2g**, **2k**, **6e** and **6f**) showed the lowest MIC value (2 µg/mL) against *Bacillus subtilis* (*B. subtilis*). In addition, compounds **2g** and **6e** displayed the strong inhibitory activity against *Enterococcus faecalis* (*E. faecalis*) with MIC values of 1 µg/mL, and compounds **2g**, **2h**, **6e** and **6f** displayed the strong inhibitory activity against *M. smegmatis* with MIC value of 4 µg/mL. Consistent with previous disk diffusion test, all the compounds showed weak activity against the Gram-negative bacteria of *E. coli* with MIC values more than 64 µg/mL. All these results indicate that these synthesized compounds only inhibit Gram-positive bacteria.

Among all the test compounds, compound **6e** showed the lowest MIC values against most of the bacteria. When the 2,4-dimethoxyphenyl group at the *N*-4 position of compound **6e** was replaced with 4-methoxyphenyl group, compound **6f** showed slightly decreased activity against *E. faecalis*. Compound **6b** with the 2-hydroxyethyl group at the *C*-6 side chain and the 2,4-dimethoxyphenyl group at the *N*-4 position showed moderate antibacterial activity against all the five tested bacteria. However, the corresponding compound **6h** with the benzyl group at the *N*-4 position was less potent than the compound **6b**. A similar phenomenon was also found between compounds **2a** and **2e**. These results suggest that the introduction of the 2,4-dimethoxyphenyl group at the *N*-4 position plays an important role in antibacterial activity, while introduction of the 4-benzyl, 4-chlorophenyl or fluorophenyl groups reduce antibacterial activity.

Side chain substituents at the *C*-6 position also affected antibacterial activity. For the carbamate derivatives **2a–k**, compound **2i** with a phenyl group was inactive, whereas the corresponding compounds **2g** and **2h** with ethyl and *i*-propyl groups, respectively, showed antibacterial activity against the tested bacteria. These results suggest that the introduction of the phenyl group at the side chain is not crucial for antibacterial activity. For the urea derivatives **6a–i** bearing the polar heterocycle ring at the side chain, compounds **6d**, **6e** and **6f** but not compound **6c**, displayed antibacterial activity to certain degree.

Table 2. Antimicrobial activity (MIC, µg/mL) of compounds **2a–b**, **2e**, **2g–2k**, **6a–f** and **6h–i**.

Compd.	MIC (µg/mL) ^a				
	<i>S. aureus</i>	<i>B. subtilis</i>	<i>E. faecalis</i>	<i>M. smegmatis</i>	<i>E. coli</i>
	ATCC 29213	ATCC 6633	ATCC 29212	ATCC 700084	ATCC 25922
2a	64	32	64	128	128
2b	64	64	64	128	128

2e	32	64	64	128	128
2g	1	2	1	4	□64
2h	2	4	4	4	□64
2k	1	2	2	32	□64
6a	4	4	8	8	□64
6b	4	8	2	8	□64
6c	16	16	16	64	□64
6d	1	4	8	8	□64
6e	1	2	1	4	□64
6f	1	2	4	4	□64
6h	4	16	8	64	□64
6i	4	32	8	64	□64
Rif ^b	≤0.0625	≤0.0625	0.5	64	8
Cip ^b	0.5	0.0625	1	0.25	≤0.0078
Van ^b	1	0.5	4	16	□64

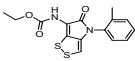
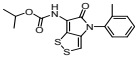
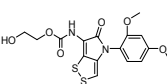
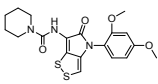
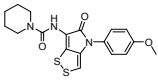
^a Minimum inhibitory concentration (MIC) was represented as the mean values of three independent experiments.

^b Used as a positive control. Rifampin (Rif), ciprofloxacin (Cip) and vancomycin (Van).

Based on the *in vitro* antibacterial activity above, five potent compounds were selected for further evaluation against four clinical isolates of rifampin-resistant *S. aureus*. As illustrated in **Table 3**, all the test compounds displayed antibacterial activity against rifampin-resistant *S. aureus* with MIC values in the range of 1-4 µg/mL, which was much lower than rifampin. In addition, compounds **6e** and **6f** exhibited similar activity as vancomycin (MIC= 1-2 µg/mL).

These results suggest that these five compounds may have different mechanism from that of rifampin to inhibit bacteria, and they might have the potential to overcome the rifampin-resistance in clinics.

Table 3. *In vitro* antibacterial activity against rifampin-resistant *S. aureus*

Compd.	Structure	MIC ($\mu\text{g/mL}$)
		Rifampin-resistant <i>S. aureus</i> (4) ^a
2g		2-4
2h		2-4
2k		2-4
6e		1-2
6f		1-2
Rifampin		>64
Vancomycin		1-2

^a Number of bacterial strains tested are given in parentheses.

2.2.3 *In vitro* Inhibitory Activity against *E. coli* RNAP and Cytotoxicity

The five most potent compounds (**2g**, **2h**, **2k**, **6e** and **6f**) and compound **6i** with weak antibacterial activity as negative control were evaluated for their inhibitory activities against *E. coli* RNAP *in vitro*. A commercially available *E. coli* RNAP assay kit was used since bacteria RNAP subunit sequences are highly conserved between Gram-positive and -negative bacteria (Irschik et al., 1983). As shown in **Table 4**, compound **6e** showed the most potent inhibitory activity against *E. coli* RNAP, with an IC_{50} value of $12.0 \pm 0.9 \mu\text{M}$ (Figure 3). Compounds **2h**, **2k** and **6f** inhibited *E. coli* RNAP with IC_{50} values of 94.4 ± 2.1 , 65.6 ± 1.2 and $87.6 \pm 1.4 \mu\text{M}$, respectively. However, compound **2g** exhibited weaker inhibitory activity against *E. coli* RNAP ($\text{IC}_{50} = 158.5 \pm 3.0 \mu\text{M}$), and compound **6i** showed no

activity against *E. coli* RNAP ($IC_{50} > 1$ mM) as expected. Moreover, the activities here were much lower than those based on the in vivo antibacterial assay (Table 3), indicating that these selected compounds might inhibit the bacterial growth through some other mechanisms in addition to the RNAP inhibition. In summary, the weaker antibacterial activity against Gram-negative bacteria than Gram-positive bacterial for these compounds might be due to the difference in cellular-uptake barriers and efflux (Kadokia et al., 2017), and the selected synthesized compounds might bind to different sites of *E. coli* RNAP from that of rifampin. Further studies are needed to reveal the exact mechanism of action.

The cytotoxicity of the selected compounds on HepG2 and LO2 cells was determined by methyl thiazoly tetrazolium (MTT) assay (Table 4). Rifampin showed no cytotoxicity against HepG2 and LO2 cells with IC_{50} value of 145.3 and 823.2 μ M, respectively. While all the selected compounds showed certain degree of cytotoxicity on both cells. In particular, compound **6e** displayed cytotoxic activity against HepG2 and LO2 cells with IC_{50} values of 6.3 and 9.8 μ M, respectively. These results suggest that we should consider the toxicity in the future for the *N*-2,4-dimethoxyphenyl dithiolopyrrolones derivatives.

Table 4. Inhibitory activity against *E. coli* RNAP and cytotoxicity of the compounds

Compounds	<i>E. coli</i> RNAP IC_{50} (μ M) ^{a, b}	Cytotoxicity IC_{50} (μ M)	
		HepG2	LO2
2g	158.5 \pm 3.0	2.0	8.3
2h	94.4 \pm 2.1	2.3	5.6
2k	65.6 \pm 1.2	1.5	2.9
6e	12.0 \pm 0.9	6.3	9.8
6f	87.6 \pm 1.4	3.4	8.6
6i	>1 mM	3.8	4.5
Rifampin	0.15 \pm 0.06	145.3	823.2

^a IC_{50} values (SD < 20%) are expressed as mean \pm SD. Each experiment was performed in triplicate.

^b The reported IC_{50} values of myxopyronin A and myxopyronin B were 20.0 μ M and 5.0 μ M, respectively (Hu et al., 1998).

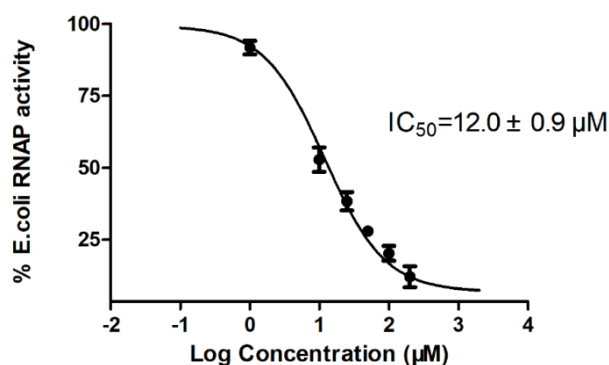


Figure 3. IC₅₀ curve for compound **6e** against *E. coli* RNAP

2.3 Biochemical Properties and Lipinski's Rule of Five (RO5) Validation

The biochemical properties of selected compounds (**2g**, **2h**, **2k**, **6e** and **6f**) were validated by free web tool (<http://www.molsoft.com/> and <http://www.swissadme.ch/>) in order to reveal the correlations between these parameters and antibacterial activity. According to the well-known RO5 (Lipinski et al, 2001) and its extensions (Keller et al, 2006), a molecular mass ≤ 500 Da, $\log P$ value ≤ 5 , hydrogen bond donors (HBD; sum of NH and OH) ≤ 5 , hydrogen bond acceptors (HBA; sum of N and O) ≤ 10 and polar surface area ≤ 140 Å² are indicative of an appropriate orally-active drug molecule for human use (Martel et al., 2016). Moreover, hydrogen bonding capacity is an important parameter for drug permeability. **Table 5** showed that all selected compounds have < 10 HBA and < 5 HBD values, and the $\log P$ and molecular weight values are less than standard values, indicating the selected compounds follow the RO5. Since lipophilic agents often demonstrate better antibacterial activity (Lipinski et al., 2001), the higher activity of compound **6e** may arise because this compound had the highest $\log P$.

Table 5. Biological properties of selected compounds.

Properties	2g	2h	2k	6e	6f
Mol. weight (g/mol)	334.04	348.06	397.03	419.10	389.09
HBA	5	5	8	6	4
HBD	1	1	2	1	2
Mol. $\log P$	3.0	3.27	1.62	3.32	3.09
SC	0	0	0	0	0

Mol. Vol (Å ³)	343.78	359.09	395.67	443.58	407.68
Mol. PSA (Å ²)	46.81	46.49	78.94	56.01	51.80
GI	high	high	high	high	high
Lipinski	0	0	0	0	0
logS	-3.37	-3.71	-2.55	-3.52	-3.44
BBB permeant	No	No	No	No	No

HBA, hydrogen bond acceptor; HBD, hydrogen bond donor; Log*P*, log partition coefficient; SC, stereo center; PSA, polar surface area; LogS, water solubility in mg/L; BBB Score, the blood-brain barrier (BBB) score (0-Low, 6-High).

2.4 Molecular Docking Studies

All the selected compounds, myxopyronin A and rifampin were docked into the switch region of bacterial RNAP (PDB ID: 3DXJ), and the binding energy was calculated by AutoDock 4.2 (Scripps Research Institute, La Jolla, CA, USA) (Morris et al., 2009). The negative and low binding energy values indicate strong interactions between the compounds and RNAP (Uddin et al., 2019). As illustrated in **Table 6**, compound **6e** in complex with RNAP had the lowest binding energy value of −8.92 kcal/mol, whereas compounds **2g**, **2h**, **2k**, **6f** and **6i** had binding energies of −7.15, −7.69, −8.44, −8.22 and −6.20 kcal/mol, respectively. **Figure 4A, C** provides the details of the specific interactions between compound **6e** and the switch region of bacterial RNAP. The methoxy group in the aromatic ring at the *N*-4 position of compound **6e** formed a hydrogen bond with Trp1038 (with a distance of 3.09 Å). In addition, the carbonyl group formed two hydrogen bonds with SER1084 and Lys621 with distance of 3.17 Å and 2.76 Å, respectively. The methoxy group in the aromatic ring of compound **6e** also interacted with LYS1463, Asp1100 and Trp1038 via a conserved water molecule (1539) within the target, which acts as a bridging molecule (**Figure 4A, C**). In addition, hydrophobic interactions between compound **6e** and Val1037, Ile1467, Val1466, Leu1053, Leu619, Gly1033 were also observed (**Figure 3C**). The results indicate that compound **6e** has an important common binding mode that is known for currently reported inhibitors of the switch region of bacterial RNAP (Mosaei and Harbottle, 2019; Sahne et al., 2013; Mukhopadhyay et al., 2008). Based on inspection of our AutoDock4.2 model, myxopyronin A was observed to have a binding energy of −8.76 kcal/mol. Rifampin binds to a site on bacterial RNAP β subunit (Irschik et al., 1983) which has no interactions with the switch region of the bacterial RNAP (binding energy

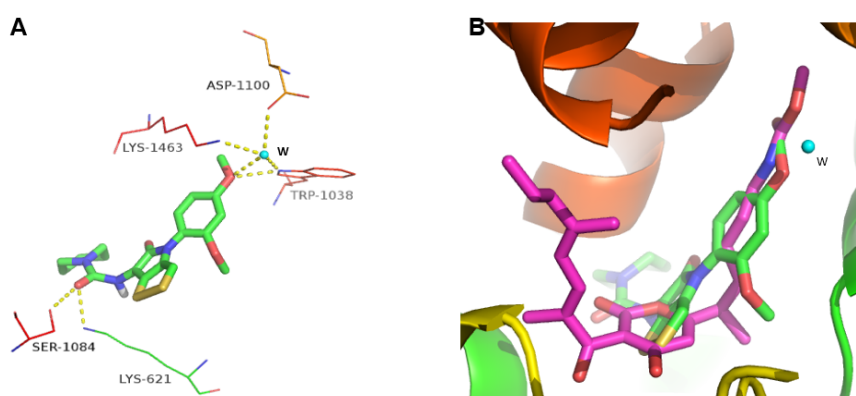
only is -2.8 kcal/mol) (Table 5). Myxopyronin A is the potent bacterial RNAP inhibitor, and adopts a U-shaped conformation that fully occupies the switch region binding pocket of RNAP (Sahner et al., 2013; Fruth et al., 2014) (Figure 4B, D). Similar to myxopyronin A, compound **6e** adopted a similar conformation in the switch region of RNAP (Figure 4B). These results suggest that compound **6e** might interact with the switch region of bacterial RNAP.

Table 6. Docking results for selected compounds into the switch region of bacterial

RNAP (PDB ID: 3DXJ).	
Compd.	Binding energy (kcal/mol) ^a
2g	-7.15
2h	-7.69
2k	-8.44
6e	-8.92
6f	-8.22
6i	-6.20
Rifampin	-2.80
Myxopyronin A ^b	-8.76

^a Binding energy, indicating binding affinity and capacity for the bacterial RNAP.

^b Myxopyronin A was used as the positive control ligand for the bacterial RNAP.



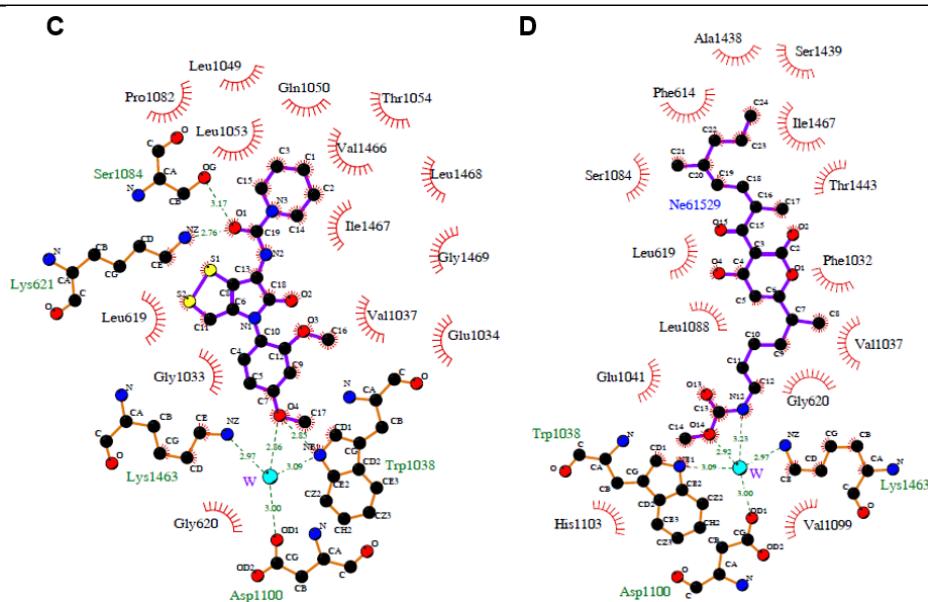


Figure 4. (A) Proposed binding mode of **6e** (green) in the switch region of bacterial RNAP; (B) Comparison of the conformation of myxopyronin A (magenta) and compound **6e** (green). W (cyan, water molecule 1539); 2D Ligand interaction diagram of compound **6e** (C) and myxopyronin A (D). Dashed lines indicate hydrogen bonds. Carbons in black, nitrogens in blue, and oxygens in red and water molecule in cyan. Figures were generated by PyMOL1.7.4 (Schrödinger, LLC, Cambridge, MA, USA) and Ligplot+v1.4.5 (European Bioinformatics Institute, London, England).

To further investigate the binding modes of the synthesized compounds with the switch region of the bacterial RNAP, molecular docking simulations of compounds **2h** and **6f** with different substituents at the *N*-4 position were also conducted. As illustrated in **Figure 5A**, the 2-methylphenyl group of compound **2h** does not form interactions with key amino acids, such as Trp1038, Asp1100 and Lys1463. Because of the absence of the polar 2-methoxy group in the aromatic ring, the docked conformation of compound **6f** in the bacterial RNAP is also different from that of compound **6e** (**Figure 5B**). This structural observation indicates that the 2-methoxy group in the aromatic ring allows the compound to properly orient within the binding site. In addition, compound **2k** with 2,4-dimethoxyphenyl group at the *N*-4 position and a different substituent at the side chain also displayed a low negative binding energy that was similar to that of compound **6e** (**Table 6**). All these data from molecular docking suggest that 2,4-dimethoxyphenyl group at the *N*-4 position of the pyrroline scaffold is crucial for high affinity binding.

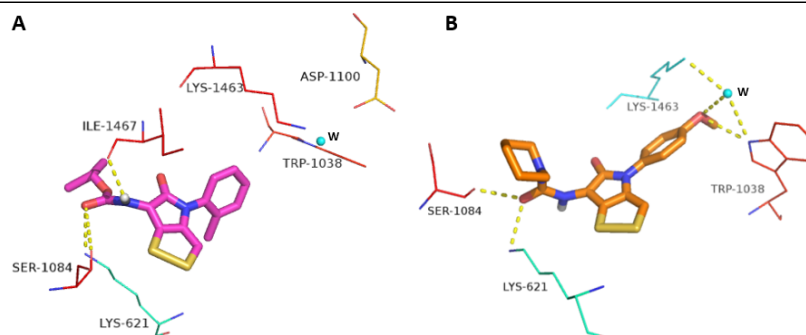


Figure 5. Proposed binding mode of **2h** (A, magenta) and **6f** (B, orange) in the switch of bacterial RNAP, W (cyan, water molecule 1539). Figures were generated by PyMOL1.7.4 (Schrödinger, LLC, Cambridge, MA, USA).

3 CONCLUSIONS

In this study, twenty *N*-aryl pyrrothine derivatives were designed, synthesized, and evaluated for the antibacterial activity. The results showed that some *N*-aryl pyrrothine derivatives have potent antimicrobial activity. Compound **6e** exhibited potent antibacterial activity against the clinical isolates of rifampin-resistant *S. aureus* and the strongest inhibitory activity against *E. coli* RNAP as well. Molecular docking studies further suggested compound **6e** interacts with the switch region of the bacterial RNAP, but further studies are required to confirm the exact binding mode. In conclusion, the *N*-aryl pyrrothine scaffold is a promising lead for antibacterial drug development.

ACKNOWLEDGMENTS

The work was funded by National Natural Science Foundation of China (No. 81660571, 81460528, 21762010), Guangxi Natural Science Foundation of China (No. 2018GXNSFAA281114, 2018GXNSFAA281135).

DATA AVAILABILITY STATEMENT

The data that supports the findings of this study are available in the supporting information of this article.

CONFLICT OF INTEREST

The authors disclose that there is no potential conflict of interest.

REFERENCES

- Campbell, E. A.; Korzheva, N.; Mustaev, A.; Murakami, K.; Nair, S.; Goldfarb, A.; Darst, S. A. (2001). Structural mechanism for rifampicin inhibition of bacterial rna polymerase. *Cell*, 104(6), 901-912.
- Chopra I. (2007). Bacterial RNA polymerase: a promising target for the discovery of new antimicrobial agents. *Current opinion in investigational drugs*, 8(8), 600-607.
- Darst, S. A. (2004). New inhibitors targeting bacterial RNA polymerase. *Trends in biochemical sciences*, 29(4), 159-160.
- Fruth, M.; Plaza, A.; Hinsberger, S.; Sahner, J. H.; Hauptenthal, J.; Bischoff, M.; Jansen, R.; Muller, R.; Hartmann, R. W.

- (2014). Binding mode characterization of novel RNA polymerase inhibitors using a combined biochemical and NMR approach. *ACS chemical biology*, 9(11), 2656-2663.
- Gao, S.; Hothersall, J.; Wu, J.; Murphy, A. C.; Song, Z.; Stephens, E. R.; Thomas, C. M.; Crump, M. P.; Cox, R. J.; Simpson, T. J.; Willis, C (2014). Biosynthesis of mupirocin by *pseudomonas fluorescens* NCIMB 10586 involves parallel pathways. *Journal of the American Chemical Society*, 136(14), 5501-5507.
- Ho, M. X.; Hudson, B. P.; Das, K.; Arnold, E.; Ebright, R. H. (2009). Structures of RNA polymerase-antibiotic complexes. *Current Opinion in Structural Biology*, 19(6), 715-723.
- Hu, T.; Schaus, J. V.; Lam, K.; Palfreyman, M. G.; Wuonola, M.; Gustafson, G.; Panek, J. S. (1998). Total synthesis and preliminary antibacterial evaluation of the RNA polymerase inhibitors (\pm)-Myxopyronin A and B. *The Journal of Organic Chemistry*, 63(7), 2401-2406.
- Irschik, H.; Gerth, K.; Hofle, G.; Kohl, W.; Reichenbach, H. (1983). The myxopyronins, new inhibitors of bacterial RNA synthesis from *Myxococcus fulvus* (Myxobacterales). *The Journal of Antibiotics*, 36(12), 1651-1658.
- Kadakia, E.; Shah, L.; Amiji, M. M. (2017). Mathematical modeling and experimental validation of nanoemulsion-based drug transport across cellular barriers. *Pharmaceutical research*, 34(7), 1416-1427.
- Keller, T. H.; Pichota, A.; Yin, Z. (2006). A practical view of 'druggability'. *Current opinion in chemical biology*, 10, 357-361.
- Li, B.; Wever, W. J.; Walsh, C. T.; Bowers, A. A. (2014). Dithiolopyrrolones: biosynthesis, synthesis, and activity of a unique class of disulfide-containing antibiotics. *Natural product reports*, 31(7), 905-923.
- Li, B.; Lyle, M. P. A.; Chen, G.; Li, J.; Hu, K.; Tang, L.; Alaoui-Jamali, M. A.; Webster, J. (2007). Substituted 6-amino-4H-[1,2]dithiol[4,3-b]pyrrol-5-ones: Synthesis, structure-activity relationships, and cytotoxic activity on selected human cancer cell lines. *Bioorganic & Medicinal Chemistry*, 15(13), 4601-4608.
- Li, C.; Sun, Y.; Wang, G.; Tan, X. (2014). Synthesis of dithiolopyrrolone derivatives and their Leukocyte-Increasing Activities. *Bulletin of the Korean Chemical Society*, 35, 3489-3494.
- Lipinski, C. A.; Lombardo, F.; Dominy, B. W.; Feeney, P. J. (2001). Experimental and computational approaches to estimate solubility and permeability in drug discovery and development settings. *Advanced Drug Delivery Reviews*, 46(1-3), 3-26.
- Ma, C.; Yang, X.; Lewis, P. J. (2016). Bacterial transcription as a target for antibacterial drug development. *Microbiology and Molecular Biology Reviews*, 80(1), 139-160.
- Maffioli, S. I.; Zhang, Y.; Degen, D.; Carzaniga, T.; Del, G. G.; Serina, S.; Monciardini, P.; Mazzetti, C.; Guglielame, P.; Candiani, G.; Chiria, A. I.; Facchetti, G.; Kaltofen, P.; Sahl, H.; Dehò, G.; Donadio, S.; Ebright, R. H. (2017). Antibacterial nucleoside-analog inhibitor of bacterial RNA polymerase. *Cell*, 169(7), 1240-1248.
- Martel, S.; Begnaud, F.; Schuler, W.; Gillerat, F.; Oberhauser, N.; Nurisso, A.; Carrupt, P. A. (2016). Limits of rapid log P determination methods for highly lipophilic and flexible compounds. *Analytica Chimica Acta*, 915, 90-101.
- Morris, G. M.; Huey, R.; Lindstrom, W.; Sanner, M. F.; Belew, R. K.; Goodsell, D. S.; Olson, A. J. (2009). AutoDock4 and AutoDockTools4: Automated docking with selective receptor flexibility. *Journal of Computational Chemistry*, 30(16), 2785-2791.
- Mosaei, H.; Harbottle, J. (2019). Mechanisms of antibiotics inhibiting bacterial RNA polymerase. *Biochemical Society*

- Mukhopadhyay, J.; Das, K.; Ismail, S.; Koppstein, D.; Jang, M.; Hudson, B.; Sarafianos, S.; Tuske, S.; Patel, J.; Jansen, R.; Irschik, H.; Eddy Arnold, E.; Ebright, R. H. (2008). The RNA polymerase "switch region" is a target for inhibitors. *Cell*, 135(2), 295-307.
- Oliva, A.; Costantini, S.; De Angelis, M.; Garzoli, S.; Bozovic, M.; Mascellino, M. T.; Vullo, V.; Ragno, R. (2018). High potency of melaleuca alternifolia Essential oil against multi-drug resistant Gram-negative bacteria and methicillin-resistant *Staphylococcus aureus*. *Molecules*, 23(10), 2584.
- Pendleton, J. N.; Gorman, S. P.; Gilmore, B. F. (2013). Clinical relevance of the ESKAPE pathogens. *Expert Review of Anti-infective Therapy*, 11(3), 297-308.
- Qin, Z.; Huang, S.; Yu, Y.; Deng, H. (2013). Dithiopyrrolone natural products: isolation, synthesis and biosynthesis. *Marine Drugs*, 11(10), 3970-3997.
- Rossolini, G. M.; Arena, F.; Pecile, P.; Rossolini, G. M.; Pollini, S. (2014). Update on the antibiotic resistance crisis. *Current Opinion in Pharmacology*, 18, 56-60.
- Sahner, J. H.; Groh, M.; Negri, M.; Hauptenthal, J. (2013). Hartmann, R. W. Novel small molecule inhibitors targeting the "switch region" of bacterial RNAP: structure-based optimization of a virtual screening hit. *European Journal of Medicinal Chemistry*, 65, 223-231.
- Tan, X.; Li, C.; Yu, Z.; Wang, P.; Nian, S.; Deng, Y.; Wu, W.; Wang, G. (2013). Synthesis of substituted 6-amino-4-(2,4-dimethoxyphenyl)-[1,2]dithiolo-[4,3-b]pyrrol-5-ones and their raising leukocyte count activities. *Chemical & Pharmaceutical Bulletin*, 61(3), 351-357.
- Thavonekham, B. (1997). A practical synthesis of ureas from phenyl carbamates. *Synthesis*, 10(7), 1189-1194.
- Uddin, R.; Zahra, N. U.; Azam, S. S. (2019). Identification of glucosyl-3-phosphoglycerate phosphatase as a novel drug target against resistant strain of *Mycobacterium tuberculosis* (XDR1219) by using comparative metabolic pathway approach. *Computational biology and chemistry*, 79, 91-102.
- Villain Guillot, P.; Bastide, L.; Gualtieri, M.; Leonetti, J. P. (2007). Progress in targeting bacterial transcription. *Drug discovery today*, 12(5-6), 200-208.
- Yakushiji, F.; Miyamoto, Y.; Kunoh, Y.; Okamoto, R.; Nakaminami, H.; Yamazaki, Y. (2013). Noguchi, N.; Hayashi, Y. Novel hybrid-type antimicrobial agents targeting the switch region of bacterial RNA polymerase. *ACS Medicinal Chemistry Letters*, 4(2), 220-224.